

Investigation on better Sensitive Silicon based MEMS Pressure Sensor for High Pressure Measurement

Suja K J

National Institute of Technology
Calicut, Kerala, India

E Surya Raveendran

Royal College of Engineering
Chingamanad , Thrissur

Rama Komaragiri

National Institute of Technology
Calicut, Kerala,India

ABSTRACT

The paper focuses on the modeling and analysis of MEMS piezoresistive pressure sensors based on shape and performance parameters. The Different shapes of diaphragms namely square, rectangular and circular diaphragms made of silicon were modeled and their performance parameters namely deflection and stress were analyzed. The simulations performed using the FEM software Intellisuite® proved that the better shape for the design of a piezoresistive pressure sensor is one with the square shaped diaphragm. The square shaped diaphragm with varying thickness is simulated and tested till their burst pressures. The work is then high lightened on the modeling of MEMS piezoresistive pressure sensors with two different square shaped diaphragms, one with silicon and the second with silicon and silicon dioxide stack using the FEM software Intellisuite®, and comparing the performance parameters of the two sensors. The diaphragm deflection in silicon pressure sensor was found to be less when compared to SOI pressure sensors, and the SOI pressure sensor is capable of giving more output voltage and exhibits more voltage sensitivity. The thickness of SOI layer plays an integral part of sensor design. Unlike the silicon pressure sensor, the SOI pressure sensor is able to operate at large pressures by changing the dimension of the diaphragm while maintaining appreciable voltage sensitivity.

General Terms

MEMS, deflection, sensitivity

Keywords

MEMS, deflection, stress, piezorsistive pressure sensor, voltage sensitivity.

1. INTRODUCTION

In recent years substantial research has been carried out on micromachined diaphragm type pressure sensors [1-5]. These sensors are fabricated by new manufacturing technologies such as bulk micromachining [6,7] or surface micromachining [8, 9]. Pressure sensors have profound applications in medical field, automobile industry, household applications, oceanography etc, [10]. Conventional transducers are bulkier and consumes more power. They are not suitable for compact and standalone systems. MEMS pressure sensors have the advantages of small size, low cost, low energy consumption and high resolution when compared to conventional transducers. Moreover MEMS technology allows more electronics to be fabricated on the same chip along with transducer to be compact and less noise design and more built-in intelligence features [11]. Diaphragms are one of most important mechanical parts for many of MEMS sensors and actuators. A thin membrane serves as the sensing element in a MEMS pressure sensors. Pressure applied on the diaphragm deflects the membrane and this deflection is limited until the

elastic force is balanced by pressure. The different shapes play a key role in the design of pressure sensors for various applications. The purpose of this paper is to analyze different shapes of diaphragms, based on the parameters namely deflection and stress using FEM software Intellisuite.

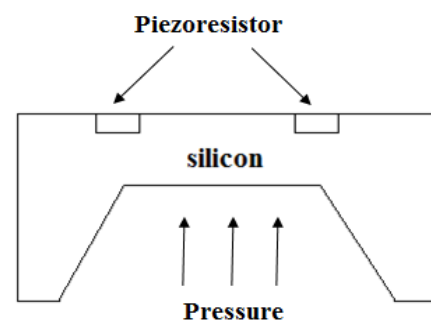


Fig. 1 Piezoresistive Silicon pressure sensor

The different MEMS materials and fabrication techniques have been under research to improve the sensitivity of piezo resistive pressure sensors. Hence the work in this paper also high light to model, compare and analyze different performance parameters like deflection, stress, output voltage and voltage sensitivity for a piezoresistive pressure sensor with the two different types of diaphragms. The diaphragm under consideration are one with conventional silicon diaphragm and other one with Silicon on Insulator (SOI) diaphragm. The SOI layer thickness of the diaphragm is varied and the effect is studied in this work. The work also extended to establish that changing dimensions of the diaphragm can make a SOI pressure sensor to withstand more stress at the edges. For large pressure ranges, the fracture stress of 7GPa, is one of the most important design criteria of pressure sensors.

2. MODELING OF DIAPHRAGMS

2.1 Deflection Analysis

Fig.1 shows the piezoresistive silicon pressure sensor. To model the silicon pressure sensor diaphragm, it is assumed that the diaphragm has a uniform thickness, with perfectly clamped edges. In the steady state, the diaphragm deflection is governed by the Lagrange equation as in eqn (1) which allows to calculate the out-of-plane membrane deflection $w(x,y)$ as a function of position [12]. In this case, cartesian coordinates are chosen for analysis as the diaphragm is rectangular in shape.

$$\frac{\partial^4 w(x,y)}{\partial x^4} + 2\alpha_{si} \frac{\partial^4 w(x,y)}{\partial x^2 \partial y^2} + \frac{\partial^4 w(x,y)}{\partial y^4} = \frac{P}{D \cdot h^3} \quad (1)$$

P represents the differential pressure applied on the membrane of thickness h , D is a rigidity parameter which depends on material properties given by eqn (2).

$$D = \frac{E h^3}{12(1-\theta^2)} \quad (2)$$

The anisotropy coefficient α_{si} , depends on the crystallographic orientation. E is the Young's modulus whereas θ is the Poisson's ratio. The factor G is called a shear modulus or Coulomb modulus and it describes the reaction of the material to the shear stress. α_{si} can be calculated using eqn (3) and eqn (4).

$$G = \frac{E}{2(1+\theta)} \quad (3)$$

$$\alpha_{si} = \theta + \frac{2G(1-\theta^2)}{E} \quad (4)$$

However the exact solution of eqn. (1) does not exist and one of the approaches used to analyze the basic shapes is the Polynomial approximation [13]. This approach is used to analyze the deflection and stress for the different shapes of diaphragms. The different diaphragms are chosen such that they have the same area. The diaphragms are analyzed for a pressure of 23.5kPa which is the applicable pressure in the linear range for a diaphragm of 10 μ m thickness. Fig. 2 shows the dimensions chosen for the various geometries of diaphragms that the diaphragm dimension are chosen in such a way that area is same for all the three diaphragms.

2.1.1 Square diaphragm

The solution to eqn. (1) for a square diaphragm with side length $\sqrt{\pi a}$ as shown in Fig.2 (a) is $w(x,y)$. With appropriate approximations and simplification the displacement of a square diaphragm $w(x,y)$ which changes with uniform pressure (P) is given by eqn (5) [13].

$$w(x,y) = \frac{1}{47} \frac{P a^4}{D} \left(\frac{1-x^2}{\pi a^2} \right)^2 \left(\frac{1-y^2}{\pi a^2} \right)^2 \quad (5)$$

The analysis is performed assuming side length (a) = 1000 μ m and diaphragm thickness (h) of 10 μ m.

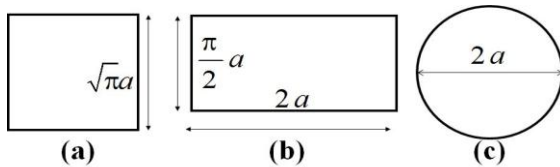


Fig. 2 Description of Diaphragms in various Dimensions

2.1.2 Rectangular Diaphragm

In case of a rectangular diaphragm the deflection in the diaphragm can be simplified as in eqn (6) [13]. The width of rectangular diaphragm is $0.5\pi a$ and a length is $2a$ as shown in Fig. 2(b)

$$w(x,y) = \frac{1}{47} \frac{P a^4}{D} \left(\frac{1-x^2}{\pi a^2} \right)^2 \left(\frac{1-y^2}{\pi a^2} \right)^2 \quad (6)$$

2.1.3 Circular Diaphragm

When considering the isotropic circular membrane which has its radius a as shown in Fig .2(c), is characterized by the axial symmetry. So in order to simplify calculations, the out-of-plane deformation $w(r)$ is considered to be dependent only on the distance from its center r and is given by eqn (7) [13].

$$w(r) = \frac{P a^4}{64 D} \left(1 - \frac{r^2}{a^2} \right)^2 \quad (7)$$

Table I gives a comparison of the theoretical results with the FEM results obtained from Intellisuite.

Table I: Comparison of deflection results for various diaphragm geometries

Shape of Diaphragm	Deflection (μ m)	
	Theoretical	Intellisuite
Square	25.10	24.87
Rectangle	22.01	21.88
Circle	31.00	30.76

From Table I, it is observed that the circular diaphragm deflects more when compared to other diaphragms.

2.2 Stress Analysis

Stress Analysis

Having computed the membrane deflection, the next important thing that has to be calculated is the stress distribution over the membrane surface. According to Hooke's law, for rectangular membrane the in-plane (XY) stress value as a function of the position on the membrane surface (x,y) may be expressed by using formulas (8) and (9) [13].

$$\sigma_x(x,y) = \frac{h.E}{2.(1-\theta^2)} \left(\frac{\partial^2 w(x,y)}{\partial x^2} + \theta \frac{\partial^2 w(x,y)}{\partial y^2} \right) \quad (8)$$

$$\sigma_y(x,y) = \frac{h.E}{2.(1-\theta^2)} \left(\frac{\partial^2 w(x,y)}{\partial y^2} + \theta \frac{\partial^2 w(x,y)}{\partial x^2} \right) \quad (9)$$

Whereas for the circular membrane the only radius dependent formula is given by:

$$\sigma(r) = - \frac{E z}{(1-\theta^2)} \left(\frac{\partial^2 w(r)}{\partial r^2} \right) \quad (10)$$

Hence stresses are relevant for the design of membrane in pressure sensors since the stresses experienced by the diaphragms at the edges should not exceed the fracture stress of silicon which is 7GPa.

For the analysis purpose the equations for stress in the x , (longitudinal stress) and the y directions, (transverse stress)

$$(5)(4)$$

which were simplified form of (8) and (9) for the various diaphragm is explained below.

2.2.1 Square diaphragm

For the square diaphragm the maximum stresses are at the centre of edges and can be shown as:

$$\sigma_x = \frac{1.02P\pi a^2}{h^2} \tag{11}$$

$$\sigma_y = \vartheta \sigma_x \tag{12}$$

2.2.2 Rectangular Diaphragm

The same is true for the rectangular diaphragm and the stresses are given by

$$\sigma_x = \frac{2Pb^2}{h^2} \frac{\frac{\pi^4 a^4}{256}}{b^4 + \frac{\pi^4 a^4}{256}} \tag{13}$$

$$\sigma_y = \vartheta \sigma_x \tag{14}$$

2.2.3 Circular Diaphragm

In circular diaphragm the maximum stresses are at the edges and are given as:

$$\sigma_r(a) = \frac{3}{4} \frac{a^2}{h^2} P \tag{15}$$

$$\sigma_t(a) = \frac{3}{4} \frac{a^2}{h^2} \vartheta P \tag{16}$$

Where σ_x and σ_y refers to longitudinal and transverse stress respectively and σ_r and σ_t are the radial and tangential stress of a circular diaphragm respectively.

Table II- Comparison of stress results for various diaphragm geometries

From the above analysis on stress, it is found that the circular diaphragm has the lowest stress at its edges when compared with the other diaphragms. It can be noted that while applying same pressure, maximum stress points were observed for a square diaphragm

3. PERFORMANCE PARAMETERS-COMPARISON AND ANALYSIS

3.1 Deflection analysis

With respect to the conditions of SSD (Small Scale Deflection) pressure values have been calculated for a 1000µm diaphragm length and for different thicknesses. The pressure values are calculated are as follows: 1.5KPa, 24 KPa, 121.1 KPa and 38 KPa for 5µm ,10µm, 15µm, and 20µm respectively. The maximum deflection is plotted for these

thicknesses and pressure values are shown in Fig.3. The FEM results are compared with the theoretical values The theoretical values are found to be in close proximity with the values from Intellisuite values which is shown in Fig.4.

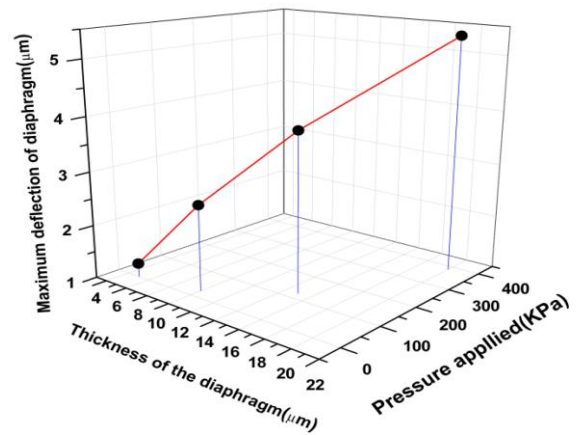


Fig. 3: Graphical representation of deflection for various thicknesses of diaphragm in SSD

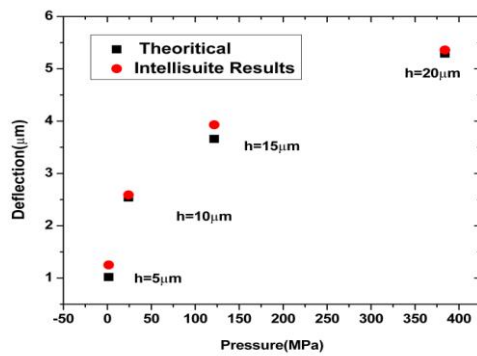


Fig. 4: Theoretical Vs FEM results for deflection

3.2 Stress analysis

Fig.5 Shows the total stress experienced by the diaphragm under different applied pressure for thicknesses 5 µm, 10 µm, 15 µm and 20µm and Fig. 6 represents the theoretical versus FEM results representing maximum stress at pressures applied to minimum thicknesses of the diaphragm.

Shape of Diaphragm	Deflection (µm)	
	Theoretical	Intellisuite
Square	236.6	235.1
Rectangle	230.2	229.1
Circle	210.4	210.0

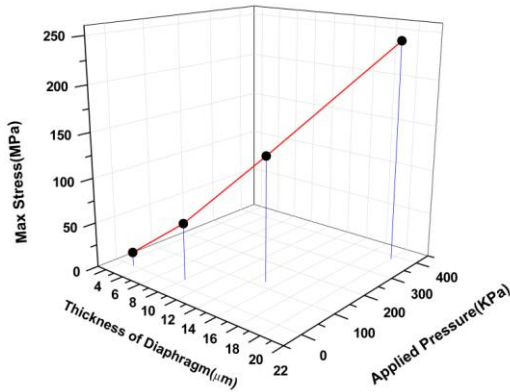


Fig. 5: Graphical representation of Stress for various thicknesses of diaphragm in SSD

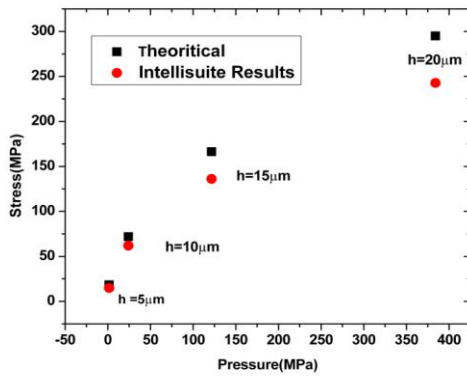


Fig 6: Theoretical Vs FEM results for stress

Thick ness (µm)	Pressure (M Pa)	Placed at boundary		Placed at the centre	
		V _{out} (mV)	S	V _{out} (mV)	S
5	0.00147	1.152	1.081	1.645	1.543
10	0.02352	6.171	0.362	8.817	0.517
15	0.12012	17.89	0.206	18.01	0.207

3.3 Sensitivity enhancement of by the relocation of piezoresistors

The Wheatstone bridge is used to measure the output voltage of the piezo resistive pressure sensor. In the absence of pressure, the bridge is balanced and the voltage output, V_o is zero. On the application of pressure to the bottom face of the piezoresistive pressure sensor diaphragm, the diaphragm gets deflected. This deflection results in a stress in the piezo resistors which in turn results in a change in the resistors dimensions. This results in a change in the resistance of the piezoresistors, there by changing its resistivity value, hence exhibiting the piezoresistive behavior. The resistors are placed where maximum stresses are being experienced. For a square diaphragm the maximum stresses are found at the center of

each edge. Hence the four resistors are placed at the edges of the diaphragms.

As shown in Fig. 7, in the Wheatstone bridge configuration, the resistors R_2 and R_3 experience a tensile stress and get elongated, thereby increasing its resistance. On the other hand, R_1 and R_4 get compressed and the value of resistance decreases. As a result, the Wheatstone bridge will be out of balance. As the output voltage is a measure of change in resistance, and the change in resistance is directly proportional to change in applied pressure, the output voltage of the Wheatstone bridge is a direct measure of applied pressure. The output voltage due to the change in resistances can be expressed as in eqn (17).

$$V_{out} = \left(\frac{R_3}{R_1 + R_3} - \frac{R_4}{R_2 + R_4} \right) V_{in} \tag{17}$$

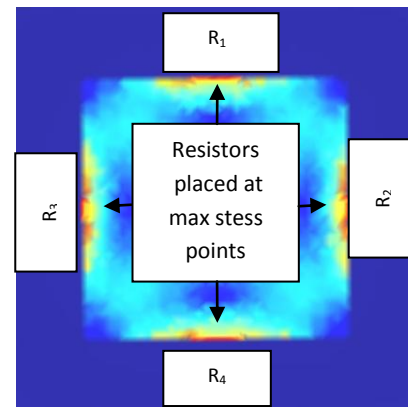


Fig 7: Placement of resistors on the pressure sensor diaphragm at maximum stress regions

Table 3 shows the output for different cases when all piezoresistors are placed at the boundary and when two piezoresistors are placed at the centre [14]. It is observed that the maximum change will occurs when the piezoresistors are placed very close to centre. From Fig 8 it can be concluded that the maximum output will not when the piezoresistors are at the boundary rather it will be maximum at some offset from the boundary.

Table III- Output voltage and sensitivity(S) for different thicknesses and for different placements of piezoresistors

From the Table III, it is clear that the placement of two piezoresistors at the centre of the diaphragm can give enhanced sensitivity but in this arrangements piezoresistors suffer from the problem of offset values. If no pressure is applied and diaphragm is placed for a long time, the bending moments and shear forces will make the diaphragm bend at the centre. This bending of the diaphragm near the centre will force change in resistance values of the piezoresistors which will be sensed by the wheat stone bridge configuration and output voltage will be generated without applying any pressure which can interpret wrong results. So this arrangement needs some proper calibration and also new methods for balancing the bridge so that without any application of pressure it can balance the wheatstone bridge and no output should generate.

Different techniques are being experimented with the Silicon diaphragm, for the design of an ocean pressure sensor, such as the double diaphragm technique, multiple diaphragm techniques where one of the diaphragm senses the low pressure ranges and the other diaphragm senses the high pressure range [15].

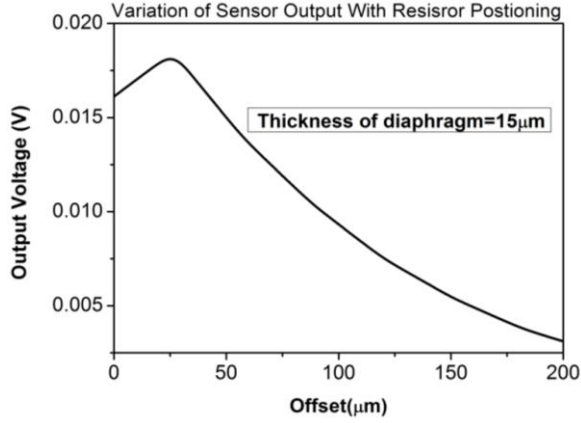


Fig 8 : Output voltage as a function of offset

4. SOI PRESSURE SENSORS

Fig. 8 shows the structural differences between the two sensors namely the silicon pressure sensor and the SOI pressure sensor.

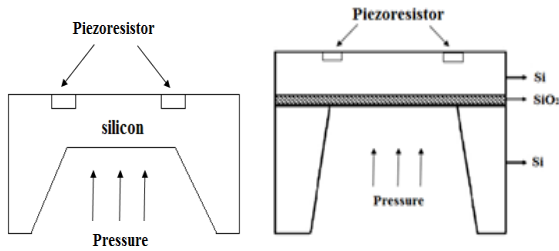


Fig 9: Basic structures of Silicon and SOI pressure sensor

The silicon pressure sensor is fabricated by bulk micromachining technology in the Si substrate. In the bulk micromachining technique, KOH solution is used to etch the silicon substrate. The wet etch forms trenches in a trapezoid shape with an angle of 54.7° as shown in Fig. 9. The remaining substrate forms diaphragm structure which deforms with applied pressure [16]. The fabrication of the SOI pressure sensor is carried out using the surface micromachining technique. Here The SOI wafer has been realized by bonded and etch back SOI (BESOI) technique [17]. Two 500μm double side polished wafers are cleaned using standard cleaning procedure. One of the wafers is then thermally oxidized to grow an oxide thickness, typically 2000Å. Both the wafers are cleaned using standard RCA1 and RCA2 cleaning to make the surfaces hydrophilic. The wafers are then brought into contact in a substrate bonder at 450 °C in vacuum. The pre bonded wafer is then annealed at 1050 °C in wet oxygen ambient for 2 hours to increase the bond strength. The bonded wafer was then etched from the bottom by 80 % KOH at 75 °C. The top side of the wafer is protected by SiO₂ as masking layer. The etching is carried out till a membrane of desired thickness is achieved thus forming the SOI diaphragm. The modeling of a SOI pressure sensor is

different from the method used for modeling the silicon pressure sensors since the buried SiO₂ layer between the substrate and the diaphragm should be considered in this model. The boundary conditions for the SOI pressure sensor remains the same as silicon pressure sensor. However there is a difference in the flexural rigidity, since the composite diaphragm is heterogeneous. The bending moment (M) in an elemental strip considered in the z-direction can be written as in eqn. (18) for SOI composite diaphragm [18].

$$M = -\int_0^{h_1} \sigma_{x1}(z-h_n) dz - \int_0^{h_1+h_2} \sigma_{x2}(z-h_n) dz \quad (18)$$

Here h_n is the distance of center of gravity from the base of the composite SOI diaphragm, h₁, h₂ are the thickness of the buried oxide and silicon layers of the composite SOI diaphragm. σ_{x1} and σ_{x2} are the normal stresses acting on the element for the buried oxide layer and silicon layer given by eqn. (19) and eqn. (20) respectively.

$$\sigma_{x1} = \left[\frac{E_1(z-h_n)}{1-\vartheta_1^2} \right] \frac{d^2 y}{dx^2} \quad (19)$$

$$\sigma_{x2} = \left[\frac{E_2(z-h_n)}{1-\vartheta_2^2} \right] \frac{d^2 y}{dx^2} \quad (20)$$

d²y/dx² is the curvature of the deflection and y is the deflection of the diaphragm in the z direction, which is assumed to be small compared to the side length (a). E₁ and E₂ are the Young's Moduli, ϑ₁ and ϑ₂ are Poisson's ratio of the buried oxide and silicon layers of the composite SOI diaphragm respectively.

Substituting σ_{x1} and σ_{x2} from eqn. (19) and (20) into eqn. (18) and performing the integration with appropriate limits results in

$$M = \left[\begin{array}{l} -\frac{E_1}{3(1-\vartheta_1^2)} \left[(h_1-h_n)^3 + h_n^3 \right] - \\ \frac{E_2}{3(1-\vartheta_2^2)} \left[(h-h_n)^3 - (h_1-h_n^3) \right] \end{array} \right] \frac{d^2 y_{SOI}}{dx^2} \quad (21)$$

Where, h=h₁+h₂, is the total thickness of the silicon-SOI composite diaphragm. Eqn (19) for bending moment (M) of an elemental strip can re-written as

$$-M = D_{SOI} \frac{d^2 y_{SOI}}{dx^2} \quad (22)$$

The flexural rigidity D_{SOI} of the stack can be written as:

$$D_{SOI} = \left[\begin{array}{l} \frac{E_1}{3.(1-\vartheta_1^2)} \left[(h_1-h_n)^3 + h_n^3 \right] \\ -\frac{E_2}{3.(1-\vartheta_2^2)} \left[(h-h_n)^3 - (h_1-h_n^3) \right] \end{array} \right] \frac{d^2 y_{SOI}}{dx^2} \quad (23)$$

The distance of center of gravity from the base of the composite diaphragm is obtained as in eqn [24].

$$h_n = \left[\frac{(E_1 h_1 Y_1) + (E_2 h_2 Y_2)}{(E_1 h_1) + (E_2 h_2)} \right] \quad (24)$$

Where

$$Y_1 = \frac{h_1}{2} \text{ and } Y_2 = h_1 + \frac{h_2}{2} \quad (25)$$

By solving eqn.(23), the modified analytical model for the small scale deflection at the center of the composite SOI diaphragm (y_{SOI}) is obtained as in eqn (26).

$$y_{SOI} = \frac{Pa^4}{4.2 \times 12} \left[\frac{E_1}{3.(1-\nu_1^2)} \left[(h_1 - h_n)^3 + h_n^3 \right] - \frac{E_2}{3.(1-\nu_2^2)} \left[(h - h_n)^3 - (h_1 - h_n^3) \right] \right]^{-1} \quad (26)$$

Hence the modeling approach for the SOI pressure sensor is different from that of the conventional silicon pressure sensor

4.1 Output Voltage Analysis

In Fig.9, the maximum deflection of a 15 μm thick diaphragm with a side length of 500μm Silicon pressure sensor is compared with the SOI pressure sensor of same dimensions. The BOX thickness is assumed to be 1.5μm. Fig 10 clearly indicates that there is an effect of SiO₂ in SOI pressure sensors. Increasing the SiO₂ thickness in SOI pressure sensor reduces the deflection of the diaphragm [19]. This is attributed to the increasing rigidity of the composite structure. The output voltage is found to be increasing in a linear fashion. The voltage output measured from the Wheatstone bridge of the two sensors revealed that more voltage output was obtained for a SOI diaphragm of side length 1000μm, in the SSD region than the Si diaphragm of side length 1000μm as shown in Fig.9.

The diaphragm in the conventional sensor is realized by bulk micromachining and the vertical and horizontal edges of the diaphragm are essentially integral part of the substrate. In contrast to this, the diaphragm in the SOI pressure sensor is realized by surface micromachining and the vertical and horizontal edges of the diaphragm are not integral part of the substrate. Also the presence of SiO₂ increases the rigidity of the structure.

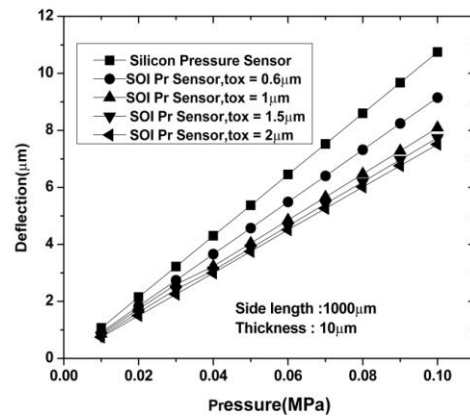


Fig.10 : Effect of thickness of buried SiO₂ in SOI pressure sensor

The output voltage is found to be increasing in a linear fashion. The voltage output measured from the Wheatstone bridge of the two sensors revealed that more voltage output was obtained for a SOI diaphragm of side length 1000μm, in the SSD region than the Si diaphragm of side length 1000μm as shown in Fig.11. The resistors in the SOI pressure sensor are dielectrically isolated from the diaphragm with the help of the buried oxide layer. This causes a very less leakage current to occur in the sensor and for which it can be made suitable to large temperature applications. Whereas in the Si pressure sensor, the pn junctions isolation allows for more current leakage and this leakage current is probable to increase as the temperature increases. Moreover the resistors in SOI pressure sensor offers higher impedance since the piezoresistors are isolated from the substrate by an insulating layer, in contrast to the bulk Si pressure sensor where leakage current exist and the impedance of the resistors is less. This accounts for higher voltage output in SOI Pressure sensor.

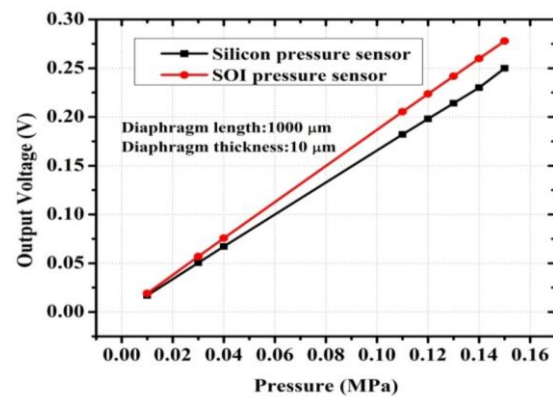


Fig 11: Voltage output of Si and SOI Pressure Sensors

4.2 Sensitivity analysis

The voltage sensitivity of the sensors with silicon and SOI diaphragm are shown in Fig.12. It is found that the voltage sensitivity of SOI pressure sensor is more than the voltage sensitivity of Si pressure sensor. This is due to fact that the output voltage of the sensor is more with increasing pressure as shown in Fig 11. It can also be observed that the voltage sensitivity is low for the conventional silicon pressure sensor in the SSD region.

a stress value of 4000MPa which is less than 7GPa as shown in Fig 13.

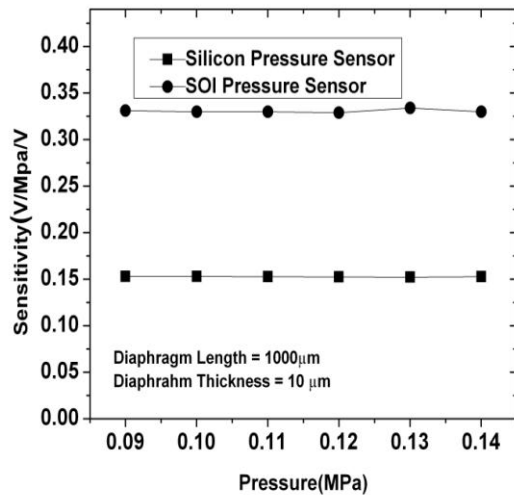


Fig 12: Sensitivity of Silicon and SOI Pressure sensors

The design criterion of the pressure sensors is that, the stress at the edges of the diaphragm should not exceed a fracture stress of 7GPa. The stresses were examined to give a maximum stress value of 6.5GPa which is well satisfied with the design criteria. This advantage can be utilized to place the resistors at the position of maximum stress available, so that maximum sensitivity can be achieved for the SOI pressure sensor, at a large pressure range. Hence this can be utilized for high pressure applications.

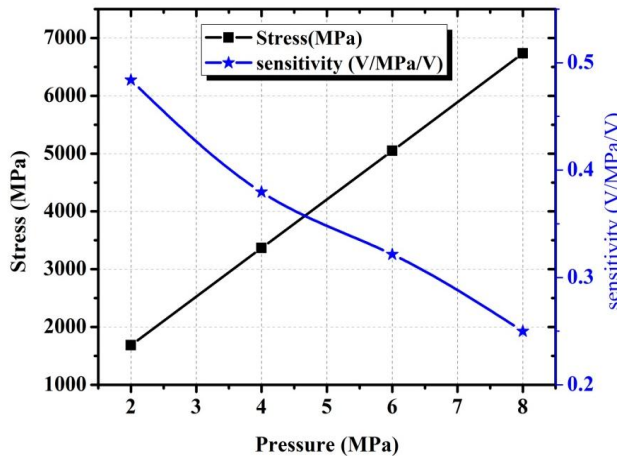


Fig 13: Voltage sensitivity of 800 side length with appropriate stress

Reducing the side length of the SOI layer diaphragm from 1000µm to 800µm with the same diaphragm thickness of 10µm has compromised the design criteria and exhibited a good voltage sensitivity in the pressure range 2-8 MPa, whereas the SOI sensor and Si pressure sensor diaphragms with side length of 1000µm would get fractured when pressures in this ranges applied [20]. Hence for a 10µm thick SOI layer diaphragm with side length 800µm can withstand to pressures in the range 2-8 MPa. The most applicable pressure at which it yields a voltage sensitivity of 0.49V/MPa/V is 2MPa and the most compromising point with the maximum stress at the edges is found to be at a pressure of 4.5 MPa with

5. CONCLUSIONS

Diaphragms of different geometries were modeled and designed for a pressure of 23.5kPa. The simulations done on the diaphragm geometries proved that circular diaphragm showed more deflection but less stress at its edges. The rectangular diaphragm on the other hand exhibited less deflection than the square diaphragm, but due to its different dimensions the stress is not uniform and equal at its edges and the stress values was greater than the square shaped diaphragm. Since the layout of circular shapes is not very common in the VLSI manufacturing, the square shaped diaphragm is considered to be a good geometry for the design of a pressure sensor. A conventional square shaped single diaphragm Silicon pressure sensor and a SOI pressure sensor were modeled and the differences in the modeling approach were analyzed. The two sensors were designed for a dimension of 1000µm and 10µm thickness. The different performance parameters like deflection, stress and voltage sensitivities were measured for the two sensors and compared. The results proved that the SOI pressure sensor exhibited less deflection and experienced less stresses at its edges, than the Silicon pressure sensors, however provided higher voltage output and sensitivity. Also changing the dimensions of the SOI pressure sensor, the stress values can be increased to a wider range of pressures until it reached the fracture stress of 7GPa, which is one of the most important design criteria. Hence SOI pressure sensors can be utilized for high pressure ranges, with better sensitivity and conventional pressure sensors can be utilized for low pressure ranges. The best range of pressure for the SOI pressure sensor with 800µm length diaphragm, which satisfies the design criteria, at a stress value of 4GPa at its edges and with a sensitivity of 0.36V/MPa/V is from 2-4.5 MPa. Moreover as SOI pressure sensors can be used for a wide range of temperatures, analysis can be performed for such designs along with temperature compensation techniques which can be extended as future work.

6. ACKNOWLEDGMENTS

The authors would like to thank the NPMASS program for funding the software tools used in this study.

7. REFERENCES

- [1] W. H. Ko, "Solid-state capacitive pressure transducers," *Sen. Actuators*, vol. 10, pp. 303–320, 1986
- [2] H. L. Chau and K. D. Wise, "Scaling limits in batch-fabricated silicon pressure sensors," *IEEE Trans. Electron Devices*, vol. ED-34, pp.850–858, 1987.
- [3] K. Suzuki, S. Suwazono, and T. Ishihara, "Cmos integrated silicon pressure sensor," *IEEE J. Solid-State Circuits*, vol. SSC-22, pp. 151–156, 1987
- [4] J. T. Kung and H.-S. Lee, "An integrated air-gap-capacitor pressure sensor and digital readout with sub-100 attofarad resolution," *IEEE J. Microelectromech. Syst.*, vol. 1, pp. 121–129, 1992.
- [5] C. H. Mastrangelo, X. Zhang, and W. C. Tang, "Surface-Micromachined capacitive differential pressure sensor with lithographically defined silicon diaphragm," *IEEE J. Microelectromech. Syst.*, vol. 5, pp. 89–105, 1996.
- [6] S. K. Clark and K. D. Wise, "Pressure sensitivity in anisotropically etched thin-diaphragm pressure sensors,"

- IEEE Trans. Electron Devices, vol. ED-26, pp.1887–1896, 1979.
- [7] H. Guckel, “surface micromachined pressure transducers,” *Sens. Actuators*, vol. A28, pp. 133–146, 1991
- [8] S. Sugiyama, K. Shimaoka, and O. Tabata, “Surface Micromachined micro-diaphragm pressure sensors,” in *Proc. 6th Int. Conf. Solid-State Sensors and Actuators (Transducers’91)*, 1991, pp. 188–191.
- [9] L. Lin, W. Yun, “MEMS pressure sensors for aerospace applications”, *Aerospace Conference, IEEE*, vol.1, March 1998, pp 429-436.
- [10] A. Mohanl, A.P. Malshel, S.Aravamudhan and S. Bhansal, “Piezoresistive MEMS Pressure Sensor and Packaging for Harsh Oceanic Environment, *Electronic Components and Technology Conference*, pp 948-950.
- [11] S. P. Timoshenko and S. Woinowsky-Krieger, “*Theory of Plates and Shells*”, 2nded., Mc Graw-Hill, New York, 1959.
- [12] A.L. Herrera-May, B.S. Soto-Cruz, F. L’opez-Huerta, and L.A. Aguilera Cort’es, “Electromechanical analysis of a piezoresistive pressure MicroMexicana de f’isica, vol. 55, No 1, Feb 2009, pp 14-24.
- [13] M.Olszacki, “Modelling and optimization of piezoresistive pressure sensors”, Ph.D.thesis, Université de Toulouse, France, July 2009.
- [14] Suja KJ, Bhanu Pratap Chowdhary, Rama Komaragiri “Study of diaphragm architecture of a MEMS pressure sensor to improve dynamic range”, IFifth ISSS Conference on MEMS, Smart Material Structures and System, September 21-22, 2012, Coimbatore, India
- [15] S. Aravamudhan, S. Bhansali, “Reinforced piezoresistive pressure sensor for ocean depth measurements,” *Sensors and Actuators A* 142 ,pp 111–117, 2008
- [16] Tai-Ran-Hsu, “MEMS& Microsystems design and manufacture”, Tata McGraw Hill, 2002.
- [17] G. S Chung, S. Kawahito, M Ishida, T Nakumura, “Novel pressure Sensors with multilayer structures”, *Electronics Letters*, vol.26, pp775-777, June 1990.
- [18] M.Narayanaswamy, R.J. Daniel, K.Sumangala, C. Jeyasehar, “Computer aided modeling and diaphragm design approach for high sensitivity silicon-on-insulator pressure sensors”, *Measurement*, vol.44, pp. 1924-1936, Sep 2011
- [19] E Surya Raveendra, Suja K J, Rama Komaragiri “Finite element analysis on miniature silicon and SOI pressure sensors “INDICON 2012, 978-1-4673-2272-0/12/\$31.00 @2012 IEEE
- [20] E Surya Raveendra, Suja K J, Rama Komaragiri “Effect of stacked Diaphragm in the MEMS Pressure Sensor for Oceanographic Applications”, ICST 2012 978-1-4577-0167-2/12/\$26.00 @2012 IEEE